



# Antibiotic-Fe<sub>3</sub>O<sub>4</sub> nanoparticles with highly efficient catalytic activity for enhanced chemiluminescence detection of tetracyclines residues in foods

Fei Yu<sup>a,1</sup>, Binghua Fan<sup>a,1</sup>, Yilin Chai<sup>b</sup>, Yue Liu<sup>c</sup>, Jiayang Wang<sup>a</sup>, Yueqi Liao<sup>a</sup>, Songcheng Yu<sup>a</sup>, Jia Wang<sup>a</sup>, Yongjun Wu<sup>a</sup>, Yilin Wang<sup>a,\*</sup>

<sup>a</sup> College of Public Health, Zhengzhou University, Henan, Zhengzhou 450001, China,

<sup>b</sup> College of Chemistry, Zhengzhou University, Henan, Zhengzhou 450001, China,

<sup>c</sup> Key Laboratory of Food Safety Quick Testing and Smart Supervision Technology for State Market Regulation, Henan, Zhengzhou 450001, China

## ARTICLE INFO

### Keywords:

Tetracyclines detection  
Fe<sub>3</sub>O<sub>4</sub> nanoparticles  
Nanozyme  
Enhanced chemiluminescence analysis

## ABSTRACT

Tetracyclines (TCs) are the most commonly antimicrobial agents that used in livestock production worldwide. It is important to supervise tetracyclines residues in food for environmental monitoring and food safety. In this study, a novel, label-free chemiluminescence (CL) assay without antibody was established. Fe<sub>3</sub>O<sub>4</sub> NPs could facilitate the CL interaction between luminol and H<sub>2</sub>O<sub>2</sub>. Interestingly, TCs could enhance the catalytic ability of Fe<sub>3</sub>O<sub>4</sub> NPs and result in a further amplification of the CL intensity. The CL intensity varied linearly with the concentration of tetracycline (TC), oxytetracycline (OTC), chlortetracycline (CTC), and ranging from 10–2400, 10–2800, and 5–2100 nmol/L, respectively; The limits of detection were 4 nmol/L for TC, 6 nmol/L for OTC, and 2 nmol/L for CTC. This CL strategy was applied successfully in testing three TCs residues in milk, eggs and honey samples with more sensitive results, which provided an alternative strategy for monitoring the correct use of TCs.

## 1. Introduction

At present, mankind is facing an unimaginable public health crisis caused by the super-resistant bacteria due to the long-term excessive and injudicious use of antibiotics (Khouly, Braun, & Chambrone, 2019). A systematic analysis about the global burden of bacterial antimicrobial resistance reported that there were estimated 4.95 million people died as a direct or indirect result of bacterial antimicrobial resistance (AMR) in 2019 and that number is expected to reach 10 million by 2050 (Murray, Ikuta, Sharara, Swetschinski, & Naghavi, 2022). It turns out that the impact of AMR on humans is intensifying (Larsen, Raisen, Ba, Sadgrove, & Larsen, 2022). Since the outbreak of COVID-19 in 2020, AMR and COVID-19 infection have mutually promoted and cross-acted, making it more difficult to treat the disease (J. Li et al., 2020; Nieuwlaat et al., 2021). In addition, the latest research found that intratumor bacterial infection plays an important role in tumor metastasis process (Fu et al., 2022).

Countries and organizations have realized the serious problems and are embarking on rigorous measures to regulate the purchase and use of antibiotics. In fact, the problem of antibiotic abuse in the animal

husbandry and breeding industry is still serious. Studies showed that more than 80% of the world's antibiotics was used in farm animals and fish aquaculture (Van Boeckel et al., 2015). Unfortunately, many countries do not have a regulatory framework on the use of antimicrobial in animals. These low-dose antibiotic residues remained in animals are continuously ingested by human through the food chain, and make the human body become a hotbed of bacterial evolution (Tu et al., 2023), posing a potential health risk. Therefore, it is important to supervise antibiotic residues in food for correcting the abuse of antibiotics in animals.

TCs were the most commonly antimicrobial agents used in the livestock industries because of its low costs and wide-range antibacterial activity. According to the World Organization for Animal Health 2019 annual report, the consumption of TCs was twice as much as that of the next highest ranked penicillin as the World Organization for Animal Health's 2019 annual report ("OIE annual report on antimicrobial agents intended for use in animals (third report)", 2019). TCs residue in various food species may have a significant impact on human health (Granados-Chinchilla & Rodríguez, 2017; Zhang et al., 2016), such as digestive system diseases (Kovtun, Averina, Alekseeva, & Danilenko,

\* Corresponding author.

E-mail address: [yilinwang90@126.com](mailto:yilinwang90@126.com) (Y. Wang).

<sup>1</sup> These authors contributed equally to this work

2020), kidney and liver damage, yellow teeth (Zhang et al., 2022) and bone growth inhibition (Ahmad, Boutros, & Hanna, 2020). To protect human health, our country has established a relatively rigorous standard for TCs residue in animal-derived food. For example, the maximized limits towards TCs residues in animal kidney, liver and muscle tissue are 0.6 mg/kg, 0.3 mg/kg and 0.2 mg/kg respectively and in eggs, milk and honey are 0.2 mg/kg. Therefore, many approaches have been developed to detect TCs residue in foods including fluorescent sensors (Liang et al., 2022), electrochemical techniques (Tran et al., 2022), electrochemiluminescent strategy (Wang, Zhu, Zhu, & Ding, 2021), high-performance liquid chromatography-tandem mass spectrometry (Melekhin et al., 2022), molecularly imprint methods (Han, Leng, Teng, Ding, & Yao, 2022) and so on. However, the disadvantages such as expensive instruments, complicated operation and time consuming have limited the application of these methods. Hence, rapid-on-site analysis, high throughput and point-of-care detection remain the focus of current research.

Chemiluminescence (CL) sensing garnered considerable interest and captured abundant imagination bolstered by sensitive, high throughput and real-time method, which has been extensively applied to drug residues detection in food (Li, Cui, Liu, Liu, & Wang, 2020; Xiu, Lu, Qi, Wang, & He, 2021). The traditional luminol-involving CL system can be promoted by the catalysts. Nano-enzyme has been developed rapidly due to its high stability, adjustable enzyme activity, diverse structures, various preparation methods, inexpensive and easy storage, and has become a powerful alternative to natural enzyme (Yang et al., 2021). In recent years, various nanozymes have been exploited to replace natural enzymes for catalytic CL system to achieve signal amplification, which further improves the stability, expands the application and reduces the cost of CL. The Fe<sub>3</sub>O<sub>4</sub> nanoparticle (MNPs) was the first reported nanozyme (Fan et al., 2017) and has been widely used in pharmacy (Wei et al., 2021), catalytic therapy (Meng et al., 2021), environmental governance (Mundekkad & Alex, 2022) and biosensing (Huang et al., 2022) due to its intrinsic peroxidase-like activity. Furthermore, TCs have a strong tendency to couple with metal ions such as Fe<sup>3+</sup>, Fe<sup>2+</sup>, Fe-TC complex can generate reactive oxygen species (ROS) (primarily ·OH) in the presence of dissolved oxygen (H. Wang, Yao, Sun, Li, & Huang, 2015). As a result, MNPs have been widely used for adsorption and removal of TCs in recent years.

Herein, a label-free CL sensor without antibody was established for the detection of TCs. MNPs can not only act as a nanozyme to catalyze chemiluminescence reactions, but also showing potential as an adsorbent. TCs could enhance the peroxidase catalytic ability of MNPs. The turn-on CL strategy enables a significant increase in sensitivity reduces the false positive rate of detection results effectively. The work was applied successfully in testing TC, OTC and CTC residues in real samples (milk, eggs and honey), which has the potential application in food security and management of health.

## 2. Material and methods

### 2.1. Reagents

Ferric chloride (FeCl<sub>3</sub>) was obtained from Sinopharm Chemical Reagent Co. TC, OTC and CTC were bought from Macklin Biochemical Co., Ltd. (Shanghai, China). Potassium chloride (KCl), calcium chloride (CaCl<sub>2</sub>), sodium hydroxide (NaOH) and sodium acetate (NaAc) came from Luoyang Chemical Reagent Factory (Luoyang, China). Casein and lactoprotein were bought from Tianjin Comio Chemical Reagent Co., Ltd. (Tianjin, China). Sucrose, α-Lactose and hydrochloric acid (HCl) were purchased from Luoyang Haohua Chemical Reagent Co., Ltd. (Luoyang, China). Penicillin, Streptomycin, Kanamycin, Naringin and tris hydroxymethyl aminomethane (Tris) came from Beijing Solaibao Technology Co., Ltd. (Beijing, China). *N, N*-dimethylformamide (DMF) was bought from Tianjin Bodi Chemical Co. Ltd. (Tianjin, China). Phenylphenol (BIP) was obtained from Shanghai Precision Biochemical

Technology Co., Ltd. (Shanghai, China). Luminol was obtained from Sigma-Aldrich Chemical Co. (St. Louis, MO). Luminol stock solution (0.01 M) was prepared in 1 M NaOH. BIP stock solution (0.35 mM) was prepared by dissolving in DMF. The chemiluminescent substrate was composed of luminol (1.4 mM), PIP (1 μM) and Tris-HCl (0.1 M, pH 9.0). All chemicals used in this study were of analytical grade without any further purification. Milli-Q ultrapure water was used throughout all the experiments.

### 2.2. Instrumentation

Morphology and structure of the MNPs were characterized by transmission electron microscopy (TEM) (JEM-2100, Japan), X-ray photoelectron spectroscopy (XPS) (Esca Lab 250Xi, Thermo Fisher Scientific, America) and Fourier transform infrared (FT-IR) (Nicolet NEXUS 470, Thermo Fisher Scientific, America). pH-meter (pH 213, HANNA, Italy) was used for pH measurements. The CL intensity (RLU) was measured by a multifunctional microporous plate reader (Spectra Max M2, Meigu Molecular Instrument Co., Ltd). Agilent 1100 liquid chromatograph was utilized to analyze tetracycline content.

### 2.3. Synthesis of Fe<sub>3</sub>O<sub>4</sub> NPs

Fe<sub>3</sub>O<sub>4</sub> NPs were synthesized by a classical solvothermal approach (Deng et al., 2005). At first, 0.5290 g of anhydrous FeCl<sub>3</sub> was dissolved in 25 mL of ethylene glycol and stirred violently to obtain clear and transparent solution. After that, 2.2582 g of anhydrous NaAc was added into the mixed solution and continued stirring for another 30 min. Subsequently, the solution was transferred into a 50 mL of Teflon-lined autoclave. The autoclave was heated at 200 °C for 8 h and then left to cooled down naturally to room temperature. The black product was collected using an external magnetic field after washing three times by anhydrous ethanol and distilled water. Finally, it was freeze-dried overnight and stored at 4 °C. The obtained Fe<sub>3</sub>O<sub>4</sub> NPs were dispersed in HAC-NaAc buffer solution for the next experiment.

### 2.4. Detection of TCs with CL method

The procedure for TCs quantitative detection is following, 10 μL of Fe<sub>3</sub>O<sub>4</sub> NPs (1.2 mg/mL) solution and 10 μL of TCs solution at different concentrations were added to low adsorption 96 microporous-plates. After incubation at ambient temperature for 5 min, 90 μL of chemiluminescent substrate and 90 μL H<sub>2</sub>O<sub>2</sub> (5 mM) were blended within each hole. The corresponding CL spectrum was recorded by multifunctional microporous plate reader within 30s.

### 2.5. Preparation of real samples

Milk, eggs and honey were chosen as actual samples to verify the assay of TCs.

**Milk:** 1 mL of milk mixed with 10 mL of pH 6.0 PBS buffer and 1 mL of 10% trichloroacetic acid solution and sonicated for 5 min. Then, the mixture was centrifuged at 3000 r/min for 10 min and the supernatant was adjusted to neutral pH with NaOH solution, filtered through 0.45 μm millipore filter and stored at 4 °C.

**Eggs:** Added 20 mL of pH 7.2 PBS buffer solution into 5 g homogenized eggs and the mixture was shook for 10 min. After static stratification, 5 mL supernatant was taken out and mixed with 5 mL PBS buffer thoroughly. The mixture was centrifuged at 5000 r/min for 1.5 min. The supernatant was filtered with 0.45 μm millipore filter and stored at 4 °C for further use.

**Honey:** 5 mL of pH 6.0 PBS buffer was added into 2.5 g of honey, then 30 mL Milli-Q water was added to the centrifuge tubes, vortex extracted for 5 min, centrifuged at 8000 r/min. The supernatant was collected and filtered by 0.45 μm millipore filter and stored at 4 °C.

Different concentrations of TCs standard solution were spiked into

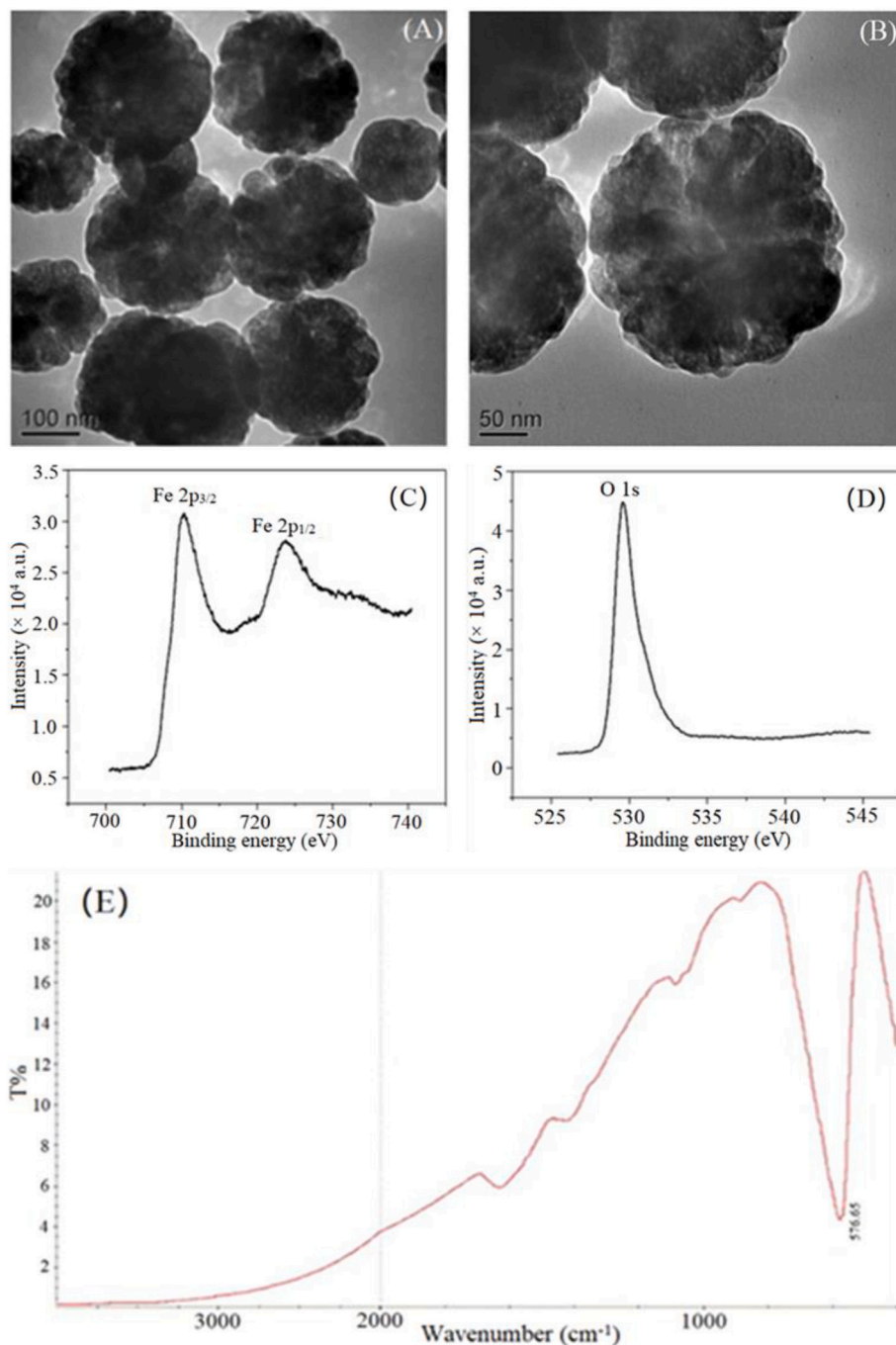


Fig. 1. Characterization of  $\text{Fe}_3\text{O}_4$  NPs. TEM images (A and B); XPS spectra (C and D) and FT-IR spectrum (E).

the actual sample samples and analyzed with the proposed process.

### 3. Results and discussions

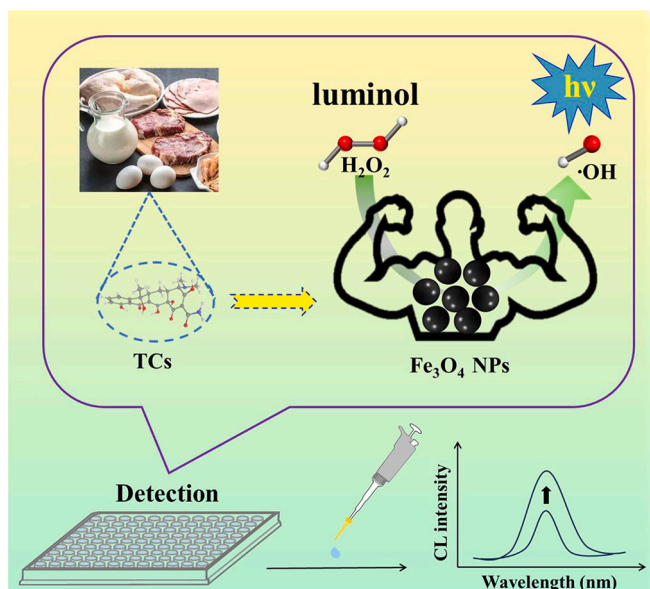
#### 3.1. Characterization of $\text{Fe}_3\text{O}_4$ NPs

The morphology and diameter of  $\text{Fe}_3\text{O}_4$  NPs were demonstrated by TEM. As can be seen in Fig. 1 A and 1B, the  $\text{Fe}_3\text{O}_4$  NPs were nearly spherical with an average diameter of approximately 250–300 nm. FTIR and XPS were used to characterize the elemental composition and chemical structure of  $\text{Fe}_3\text{O}_4$  NPs. Notably, in the XPS spectra Fe 2p (Fig. 1C), the peaks at 710 and 725 eV corresponded to Fe 2p<sub>1/2</sub> and Fe 2p<sub>3/2</sub>, respectively. The binding energies of O1s was found to be about 530 eV (Fig. 1D). The FT-IR spectra was shown in Fig. 1E, with an

absorption peak at 576.65  $\text{cm}^{-1}$ , which is characteristic of the Fe–O bond. All the above characterizations distinctly proved the successful synthesis of  $\text{Fe}_3\text{O}_4$  NPs.

#### 3.2. Sensing mechanism for assay of TCs

$\text{Fe}_3\text{O}_4$  NPs have been proved to have excellent peroxidase-like activity and they can catalyze the decomposition of  $\text{H}_2\text{O}_2$  generating hydroxyl radicals ( $\cdot\text{OH}$ ) by Fenton reaction ( $\text{Fe}^{2+}/\text{Fe}^{3+} + \text{H}_2\text{O}_2$ ) (Jaafarzadeh et al., 2018; X. Wei, Xie, Wang, & Yang, 2020). In addition, TCs have a strong tendency to interact with metal ions such as  $\text{Fe}^{3+}$ ,  $\text{Fe}^{2+}$ , and Fe–TC complex can generate reactive oxygen species (ROS) (primarily  $\cdot\text{OH}$ ) in the presence of dissolved oxygen (Liu et al., 2022; H. Wang et al., 2015). More interestingly, TCs could enhance the



**Scheme 1.** The principle of TCs detection based on enzyme-like activity of  $\text{Fe}_3\text{O}_4$  NPs.

peroxidase catalytic ability of Fe-based nanomaterial (Z. Li et al., 2023). As shown in Scheme 1, firstly,  $\text{Fe}_3\text{O}_4$  NPs could catalyze the decomposition of  $\text{H}_2\text{O}_2$  to produce  $\cdot\text{OH}$  radicals, and  $\cdot\text{OH}$  could oxidize luminol to produce luminescence. The transfer of electrons in the  $\text{Fe}_3\text{O}_4$  NPs may be accelerated by the TCs, which result in the enhancement of peroxidase catalytic ability. As expected, through the complexation of TCs, the  $\text{Fe}_3\text{O}_4$  NPs exhibited superior catalytic properties, leading to an enhanced CL intensity.

### 3.3. The feasibility for TC detection using CL method

To figure out the effect of TCs on the CL system, the CL spectra and kinetic curve of luminol- $\text{H}_2\text{O}_2$ - $\text{Fe}_3\text{O}_4$  NPs with or without TCs were investigated (shown in Fig. 2(A) and 2(B)). It was clearly that TCs could significantly enhance the CL intensity of the system luminol- $\text{H}_2\text{O}_2$ - $\text{Fe}_3\text{O}_4$  NPs. The maximum emission wavelengths of luminol- $\text{H}_2\text{O}_2$ - $\text{Fe}_3\text{O}_4$  NPs-TCs were still near 425 nm, which was same as the luminol- $\text{H}_2\text{O}_2$  system. The CL intensity of the system reached a maximum at the beginning of the reaction and began to weaken rapidly, and decayed to a relatively stable state after 1 min. It indicated that  $\text{Fe}_3\text{O}_4$  NPs and TCs acted as the cocatalysts to enhance CL intensity of luminol- $\text{H}_2\text{O}_2$  system without changing its reaction mechanism. All of these confirmed this enhanced CL system could be applied successfully in the detection of TCs.

To verify the feasibility of this method, four groups of experiments were designed using CTC as objective, and each group included the sample test (with CTC) and blank test (without CTC). The CL intensity in

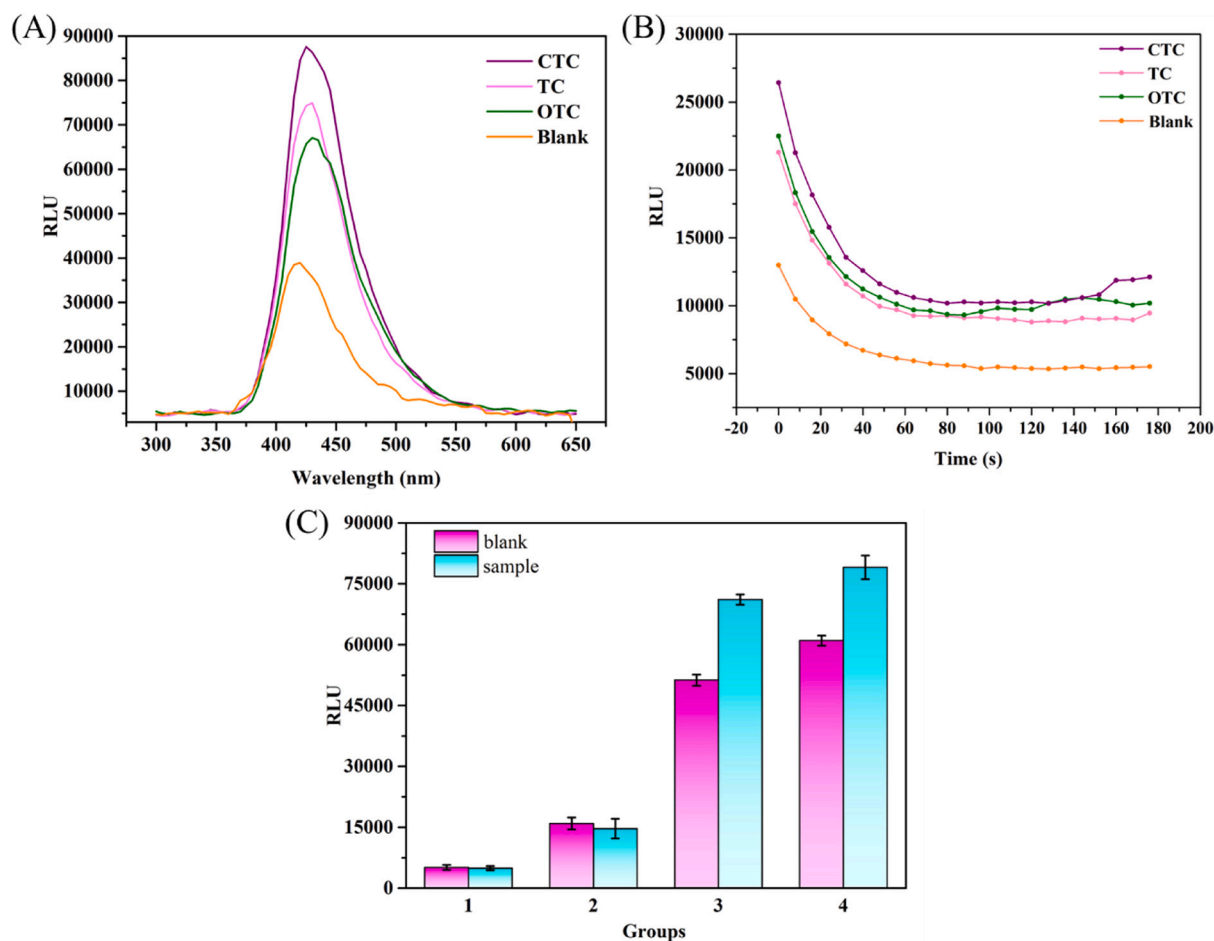


**Fig. 2.** The feasibility of CL analysis. (A) The CL spectra of luminol- $\text{H}_2\text{O}_2$ - $\text{Fe}_3\text{O}_4$  NPs with or without TCs. (B) The CL kinetic curve of luminol- $\text{H}_2\text{O}_2$ - $\text{Fe}_3\text{O}_4$  NPs with or without TCs. (C) The enhancement effect of  $\text{Fe}_3\text{O}_4$  NPs and CTC on the system of luminol- $\text{H}_2\text{O}_2$  (Group I: luminol- $\text{H}_2\text{O}_2$  with or without CTC; Group II: luminol- $\text{H}_2\text{O}_2$ -BIP with or without CTC; Group III:  $\text{Fe}_3\text{O}_4$  NPs-luminol- $\text{H}_2\text{O}_2$  with or without CTC; Group IV:  $\text{Fe}_3\text{O}_4$  NPs-luminol- $\text{H}_2\text{O}_2$ -BIP with or without CTC;).

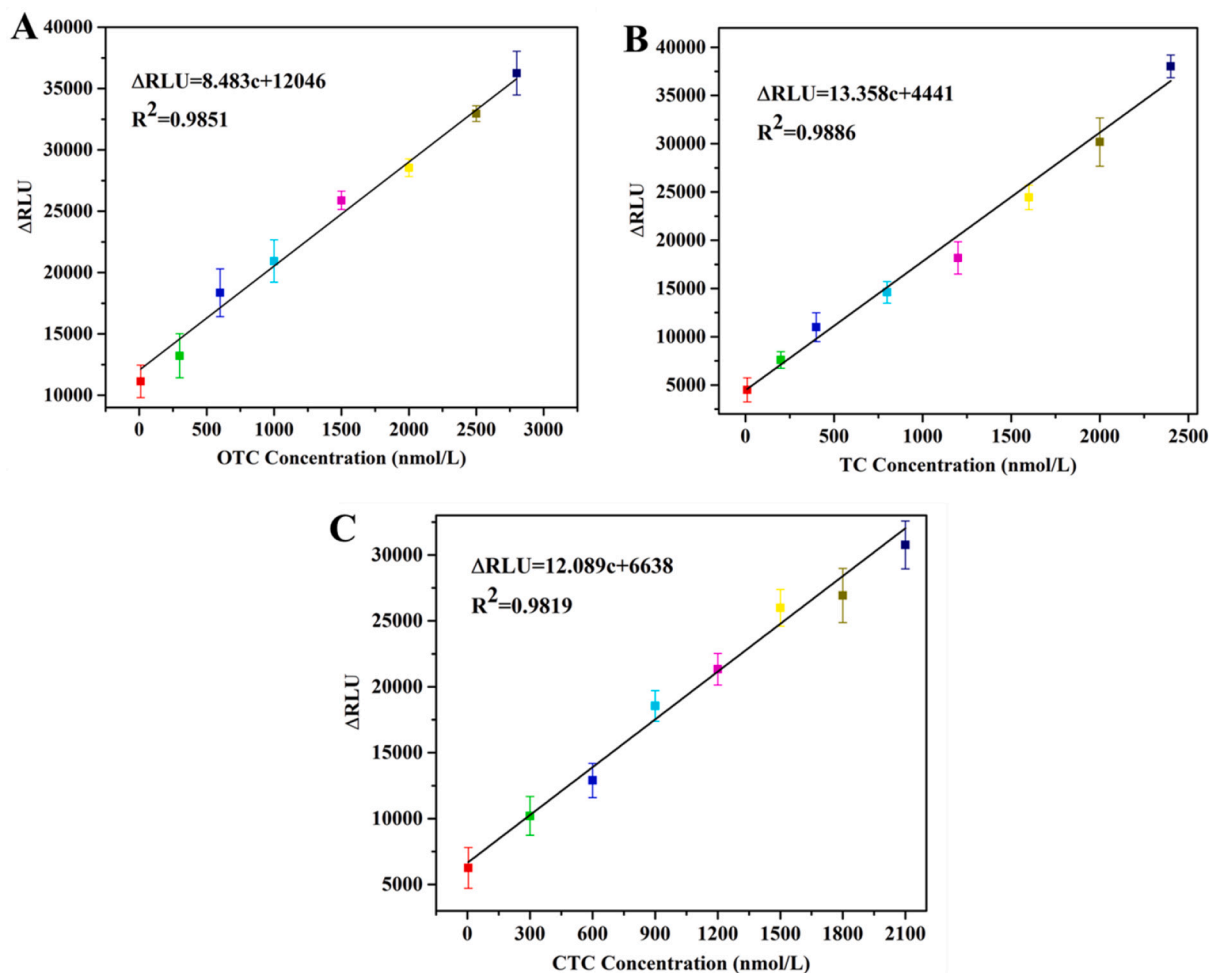


Fig. 3. Linear relationship between  $\Delta$ RLU intensity and different concentration of TCs. (A is for CTC; B is for TC; C is for OTC)

the sample test and the blank test were measured simultaneously. In addition, BIP, which was commonly used to prolong the CL time and enhance the CL intensity by improving the stability of hydroxy radicals. As shown in Fig. 2(C), the CL intensity of group II and group III was greater than that of group I and group IV, which indicated that the CL intensity of the system of luminol- $H_2O_2$  was enhanced in the presence of  $Fe_3O_4$  NPs due to their enzyme-like activity. The catalytic ability is ranked as BIP=BIP-CTC <  $Fe_3O_4$  NPs <  $Fe_3O_4$  NPs-CTC <  $Fe_3O_4$  NPs-CTC-BIP. The enhanced CL behavior is due to the complexation of  $Fe_3O_4$  NPs with CTC.

### 3.4. Optimization of experimental conditions

To achieve the optimal analytical results, four critical parameters such as the concentrations of  $Fe_3O_4$  NPs,  $H_2O_2$ , luminol and the pH of buffer solution were optimized. The CL intensity of sample test (RLU) and blank test (RLU<sub>0</sub>) in each group were measured simultaneously. As shown in Fig. S1, with the increasing of the concentration of  $Fe_3O_4$  NPs, the change of CL intensity ( $\Delta$ RLU = RLU-RLU<sub>0</sub>) increased at the beginning, and reached a maximum at 1.2 mg/mL. Therefore, 1.2 mg/mL of  $Fe_3O_4$  NPs was employed in following study. Similarly, the concentration of  $H_2O_2$  and luminol were optimized as 20 mmol/L and 3 mmol/L (Fig. S2 and S3). Likewise, the influence of different pH of the

Table 1  
Comparison of different methods for the determination of TCs.

Detection method for TCs	Detection range (nmol/L)			Limit of detection (LOD) (nmol/L)			Ref.
	TC	OTC	CTC	TC	OTC	CTC	
CL method	10–2400	10–2800	5–2100	4.0	6.0	2.0	This work
HPLC	300–1600	300–1800	300–1700	150	150	150	This work
ELISA		0.58–4.5		1.62	7.2	14.4	(Chen et al., 2015)
Ratio fluorescence	$10^{-10^4}$	–	–	5.0	–	–	(Zhang et al., 2022)
MOF-fluorescent	$0-2 \times 10^4$	$0-2 \times 10^4$	$0-2 \times 10^4$	65	390	92	(Wang et al., 2022)
Fluorescence	–	25–1750	–	–	9.5	–	(Y. Wang et al., 2018)
CDs-fluorescent		$100-5 \times 10^4$			41.7		(Tang, Wang, Ye, Zhao, & Zhao, 2022)
Nanozyme-Colorimetry	100–1000	50–1000	–	45	26	–	(Z. Li et al., 2023)
AuNP-colorimetry	$945-2.9 \times 10^4$	$912-3.5 \times 10^4$	$815-2.5 \times 10^4$	45.0	43.4	38.8	(Shen, Chen, Li, He, & Li, 2014)
DNAzyme-colorimetry	11–1000	10.3–1000	10.6–1000	3.3	3.1	3.2	(Tang et al., 2022)

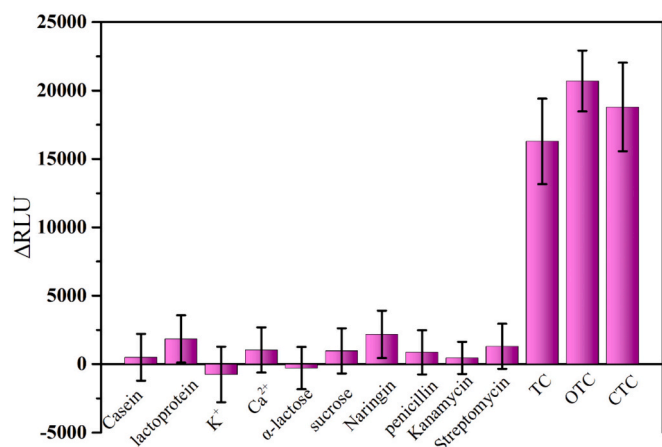


Fig. 4. Selectivity of the CL method,  $n = 3$ .

solution has been also studied (Fig. S4). It can be seen that the CL intensity increased to the maximum at pH 9.0, implying that  $\text{Fe}_3\text{O}_4$  NPs might display the higher catalytic activity at alkaline condition.

### 3.5. Analytical performance of the CL method

Under the optimal conditions, the CL intensity of different concentrations of TCs were measured using the proposed method. As shown in Fig. 3, the linear relationship between the  $\Delta\text{RLU}$  and OTC concentration was observed in the range of 10–2800 nmol/L. The linear regression equation was  $\Delta\text{RLU} = 8.483c + 12,046$  ( $R^2 = 0.9851$ ). The calculated limit of detection (LOD) was assessed to be 6 nmol/L. Accordingly, there was a good linear correlation between  $\Delta\text{RLU}$  and TC in the range of 10–2400 nmol/L. The linear regression equation was  $\Delta\text{RLU} = 13.358c + 4441$  ( $R^2 = 0.988$ ), the LOD was calculated as 4 nmol/L. For CTC. The linear regression equation was  $\Delta\text{RLU} = 12.089c + 6638$  ( $R^2 = 0.9819$ ) in the range of 5–2100 nmol/L. The LO was assessed to be 2 nmol/L. Compared with other methods (Table 1), this sensing strategy had a relatively lower LOD and a wide detection range than most methods previously reported in literatures as well as the HPLC methods developed by ourselves for validation.

### 3.6. Selectivity for TCs

To assess the selectivity of the proposed CL method, several usual interferents were performed, such as antibiotics, molecules and ions. As shown in Fig. 4, only three TCs could result in a significant enhancement of the CL intensity. There were no changes in CL intensity with other interfering substances, indicating that this method had an outstanding specificity for TCs detection.

### 3.7. Real samples analysis

To further validate the reliability of the proposed method in real samples analysis, we performed the detections of TCs in milk, eggs and honey. The sample pretreatment was processed according to the method in 2.5. As no TCs were measured in these real samples using the HPLC method, recovery experiments were used to assess the applicability of the assay in real samples. As presented in Table S1, the results suggested a satisfactory recovery of spiked samples ranged from 92.9%–110.0% (milk), 92.9%–110.0% (eggs), and 92.9%–104.2% (honey), which were much better than that of HPLC. The RSDs were 4.8%–9.0% (milk), 4.1%–8.2% (eggs), 5.1%–8.8% (honey), respectively. All the above results indicated this CL method was qualified to detect TCs in milk, eggs and honey.

## 4. Conclusions

In summary, a highly sensitive and simple CL method has been proposed for TCs detection using the enzyme-like activity of  $\text{Fe}_3\text{O}_4$  NPs. Compared with the HPLC method for TCs detection, the CL method is rapid, low-cost, simple in materials and does not require costly equipment or specialized experts. The presence of TCs is revealed by the increased CL intensity at 425 nm as the TCs concentration increases. As shown in Table 1, the detection limit of this constructed label-free CL assay is better in comparison to other recently developed spectral sensors, such as fluorescence sensors and colorimetric sensors. Together with its extensive linear range and relatively low LOD, this CL method has the potential application in food security and management of health with the following advantages. First, the proposed sensing strategy is broadly specific for the TCs family of antibiotics and is suitable for detecting the sum of TCs residues. Second, the CL sensor operates without the need for bioreceptors, and the reaction time is as short as 30 s, which is a significant advantage for on-site screening of TCs in practical applications. Third, compared with most “turn-off” sensors, the increase of signal reduces the false positive rate of detection results effectively. This study offers a new broad-spectrum sensing strategy for TCs detection, providing a viable alternative for on-the-spot ultrarapid screening of TCs residues.

## Supporting Information

Supporting Information is available from the Wiley Online Library or from the author.

## Author contributions

F. Yu and Y. Wang conceived and designed the principle of the research; B. Fan and Y. Chai performed the experiments and research; Jiaxiang Wang and Y. Liao fabricated and characterized the  $\text{Fe}_3\text{O}_4$  NPs; Jia Wang and S. Yu analyzed data; F. Yu and Y. Wang wrote the article; Yue. Liu and Y. Wu supervised the work. Every author has approved the final manuscript.

## CRediT authorship contribution statement

**Fei Yu:** Writing – original draft, Methodology. **Binghua Fan:** Methodology, Investigation. **Yue Liu:** Supervision. **Jiaxiang Wang:** Software. **Yueqi Liao:** Investigation. **Songcheng Yu:** Validation. **Jia Wang:** Methodology. **Yongjun Wu:** Supervision, Conceptualization. **Yilin Wang:** Software, Resources.

## Declaration of competing interest

The authors declare that they have no known competing financial interests or personal relationships that could have appeared to influence the work reported in this paper.

## Data availability

No data was used for the research described in the article.

## Acknowledgements

This work was financially supported by Natural Science Foundation of Henan Province [grant number 222300420302]; National Natural Science Foundation of China [grant number 82204100].

## Appendix A. Supplementary data

Supplementary data to this article can be found online at <https://doi.org/10.1016/j.fochx.2024.101485>.

## References

- Ahmad, Y., Boutros, H., & Hanna, K. (2020). Out of the blue: A case of blue subungual discoloration associated with prolonged tetracycline use. *Cureus*, 12(4), Article e7810. <https://doi.org/10.7759/cureus.7810>
- Chen, Y., Kong, D., Liu, L., Song, S., Kuang, H., & Xu, C. (2015). Development of an ELISA and immunochromatographic assay for tetracycline, oxytetracycline, and chlortetracycline residues in milk and honey based on the class-specific monoclonal antibody. *Food Analytical Methods*, 9(4), 905–914. <https://doi.org/10.1007/s12161-015-0262-z>
- Deng, H., Li, X., Peng, Q., Wang, X., Chen, J., & Li, Y. (2005). Monodisperse magnetic single-crystal ferrite microspheres. *Angewandte Chemie International Edition*, 44(18), 2782–2785. <https://doi.org/10.1002/anie.200462551>
- Fan, K., Wang, H., Xi, J., Liu, Q., Meng, X., Duan, D., Gao, L., & Yan, X. (2017). Optimization of Fe<sub>3</sub>O<sub>4</sub> nanozyme activity via single amino acid modification mimicking an enzyme active site. *Chemical Communications*, 53(2), 424–427. <https://doi.org/10.1039/c6cc08542c>
- Fu, A., Yao, B., Dong, T., Chen, Y., Yao, J., Liu, Y., Li, H., Bai, H., Liu, X., Zhang, Y., Wang, C., Guo, Y., Li, N., & Cai, S. (2022). Tumor-resident intracellular microbiota promotes metastatic colonization in breast cancer. *Cell*, 185(8), 1356–1372. <https://doi.org/10.1016/j.cell.2022.02.027>
- Granados-Chinchilla, F., & Rodríguez, C. (2017). Tetracyclines in food and feedingstuffs: From regulation to analytical methods, bacterial resistance, and environmental and health implications. *Journal of Analytical Methods in Chemistry*, 2017, Article 1315497. <https://doi.org/10.1155/2017/1315497>
- Han, S., Leng, Q., Teng, F., Ding, Y., & Yao, A. (2022). Preparation of mesh covalent organic framework Tpa-2-based adsorption enhanced magnetic molecularly imprinted composite for selective extraction of tetracycline residues from animal-derived foods. *Food Chemistry*, 384, Article 132601. <https://doi.org/10.1016/j.foodchem.2022.132601>
- Huang, Y., Gu, Y., Liu, X., Deng, T., Dai, S., Qu, J., ... Qu, L. (2022). Reusable ring-like Fe<sub>3</sub>O<sub>4</sub>/Au nanozymes with enhanced peroxidase-like activities for colorimetric-SERS dual-mode sensing of biomolecules in human blood. *Biosensors and Bioelectronics*, 209, Article 114253. <https://doi.org/10.1016/j.bios.2022.114253>
- Jaafarzadeh, N., Takdastan, A., Jorfi, S., Ghanbari, F., Ahmadi, M., & Barzegar, G. (2018). The performance study on ultrasonic/Fe<sub>3</sub>O<sub>4</sub>/H<sub>2</sub>O<sub>2</sub> for degradation of azo dye and real textile wastewater treatment. *Journal of Molecular Liquids*, 256, 462–470. <https://doi.org/10.1016/j.molliq.2018.02.047>
- Khouly, I., Braun, R. S., & Chamberone, L. (2019). Antibiotic prophylaxis may not be indicated for prevention of dental implant infections in healthy patients. A systematic review and meta-analysis. *Clinical Oral Investigations*, 23(4), 1525–1553. <https://doi.org/10.1007/s00784-018-2762-x>
- Kovtna, A. S., Averina, O. V., Alekseeva, M. G., & Danilenko, V. N. (2020). Antibiotic resistance genes in the gut microbiota of children with autistic spectrum disorder as possible predictors of the disease. *Microbial Drug Resistance*, 26(11), 1307–1320. <https://doi.org/10.1089/mdr.2019.0325>
- Larsen, J., Raisen, C. L., Ba, X., Sadgrove, N. J., & Larsen, A. R. (2022). Emergence of methicillin resistance predates the clinical use of antibiotics. *Nature*, 602(7895), 135–141. <https://doi.org/10.1038/s41586-021-04265-w>
- Li, J., Wang, J., Yang, Y., Cai, P., Cao, J., Cai, X., & Zhang, Y. (2020). Etiology and antimicrobial resistance of secondary bacterial infections in patients hospitalized with COVID-19 in Wuhan, China: A retrospective analysis. *Antimicrobial Resistance & Infection Control*, 9(1), 153. <https://doi.org/10.1186/s13756-020-00819-1>
- Li, Z., Meng, F., Li, R., Fang, Y., Cui, Y., Qin, Y., & Zhang, M. (2023). Amino-functionalized Fe(III)-based MOF for the high-efficiency extraction and ultrasensitive colorimetric detection of tetracycline. *Biosensors and Bioelectronics*, 234, Article 115294. <https://doi.org/10.1016/j.bios.2023.115294>
- Li, Z. B., Cui, P. L., Liu, J., Liu, J. X., & Wang, J. P. (2020). Production of generic monoclonal antibody and development of chemiluminescence immunoassay for determination of 32 sulfonamides in chicken muscle. *Food Chemistry*, 311, Article 125966. <https://doi.org/10.1016/j.foodchem.2019.125966>
- Liang, N., Hu, X., Li, W., Wang, Y., Guo, Z., Huang, X., Li, Z., Zhang, X., Zhang, J., Xiao, J., Zou, X., & Shi, J. (2022). A dual-signal fluorescent sensor based on MoS<sub>2</sub> and CdTe quantum dots for tetracycline detection in milk. *Food Chemistry*, 378, Article 132076. <https://doi.org/10.1016/j.foodchem.2022.132076>
- Liu, S., Wang, J., Hu, Y., Shi, Y., Yang, J., & Zhang, M. (2022). Differential sensing of antibiotics using metal ions and gold nanoclusters based on TMB-H<sub>2</sub>O<sub>2</sub> system. *Chemosensors*, 10(6), 222. <https://doi.org/10.3390/chemosensors10060222>
- Melekhin, A. O., Tolmacheva, V. V., Goncharov, N. O., Apyari, V. V., Dmitrienko, S. G., Shubina, E. G., & Grudev, A. I. (2022). Multi-class, multi-residue determination of 132 veterinary drugs in milk by magnetic solid-phase extraction based on magnetic hypercrosslinked polystyrene prior to their determination by high-performance liquid chromatography-tandem mass spectrometry. *Food Chemistry*, 387, Article 132866. <https://doi.org/10.1016/j.foodchem.2022.132866>
- Meng, X., Li, D., Chen, L., He, H., Wang, Q., Hong, C., He, J., Gao, X., Yang, Y., Jiang, B., Nie, C., Yan, X., Gao, L., & Fan, K. (2021). High-performance self-cascade pyrite nanozymes for apoptosis-ferroptosis synergistic tumor therapy. *ACS Nano*, 15(3), 5735–5751. <https://doi.org/10.1021/acsnano.1c01248>
- Mundekkad, D., & Alex, A. V. (2022). Analysis of structural and biomimetic characteristics of the green-synthesized Fe<sub>3</sub>O<sub>4</sub> nanozyme from the fruit peel extract of punica granatum. *Chemical Papers*, 76(6), 3863–3878. <https://doi.org/10.1007/s11696-022-02130-2>
- Murray, C. J. L., Ikuta, K. S., Sharara, F., Swetschinski, L., & Naghavi, M. (2022). Global burden of bacterial antimicrobial resistance in 2019: A systematic analysis. *The Lancet*, 399(10325), 629–655. [https://doi.org/10.1016/s0140-6736\(21\)02724-0](https://doi.org/10.1016/s0140-6736(21)02724-0)
- Nieuwlaat, R., Mbuagbaw, L., Mertz, D., Burrows, L. L., Bowdish, D. M. E., Moja, L., ... Schünemann, H. J. (2021). Coronavirus disease 2019 and antimicrobial resistance: Parallel and interacting health emergencies. *Clinical Infectious Diseases*, 72(9), 1657–1659. <https://doi.org/10.1093/cid/ciaa773>
- OIE. (2019). OIE annual report on antimicrobial agents intended for use in animals (third report). [http://www.oie.int/fileadmin/Home/eng/Our\\_scientific\\_expertise/docs/pdf/AMR/Annual\\_Report\\_AMR\\_3.pdf](http://www.oie.int/fileadmin/Home/eng/Our_scientific_expertise/docs/pdf/AMR/Annual_Report_AMR_3.pdf) (Available online at: OIE. accessed December 19, 2023).
- Shen, L., Chen, J., Li, N., He, P., & Li, Z. (2014). Rapid colorimetric sensing of tetracycline antibiotics with in situ growth of gold nanoparticles. *Analytica Chimica Acta*, 839, 83–90. <https://doi.org/10.1016/j.aca.2014.05.021>
- Tang, X., Wang, L., Ye, H., Zhao, H., & Zhao, L. (2022). Biological matrix-derived carbon quantum dots: Highly selective detection of tetracyclines. *Journal of Photochemistry and Photobiology A: Chemistry*, 424, Article 113653. <https://doi.org/10.1016/j.jphotochem.2021.113653>
- Tang, Y., Huang, X., Wang, X., Wang, C., Tao, H., & Wu, Y. (2022). G-quadruplex DNAzyme as peroxidase mimetic in a colorimetric biosensor for ultrasensitive and selective detection of trace tetracyclines in foods. *Food Chemistry*, 366, Article 130560. <https://doi.org/10.1016/j.foodchem.2021.130560>
- Tran, T. T., Do, M. N., Dang, T. N. H., Tran, Q. H., Le, V. T., Dao, A. Q., & Vasseghian, Y. (2022). A state-of-the-art review on graphene-based nanomaterials to determine antibiotics by electrochemical techniques. *Environmental Research*, 208, Article 112744. <https://doi.org/10.1016/j.envres.2022.112744>
- Tu, Z., Shui, J., Liu, J., Tuo, H., Zhang, H., Lin, C., Feng, J., Feng, Y., Su, W., & Zhang, A. (2023). Exploring the abundance and influencing factors of antimicrobial resistance genes in manure plasmidome from swine farms. *Journal of Environmental Science*, 124, 462–471. <https://doi.org/10.1016/j.jes.2021.11.030>
- Van Boeckel, T. P., Brower, C., Gilbert, M., Grenfell, B. T., Levin, S. A., Robinson, T. P., ... Laxminarayan, R. (2015). Global trends in antimicrobial use in food animals. *Proceedings of the National Academy of Sciences*, 112(18), 5649–5654. <https://doi.org/10.1073/pnas.1503141112>
- Wang, C., Ren, G., Zhou, S., Yang, Y., Sun, A., Fang, Y., ... Pan, Q. (2022). Heteronuclear metal-organic framework-based fluorescent sensor for the detection of tetracycline antibiotics. *Applied Organometallic Chemistry*, 36(8), Article e6767. <https://doi.org/10.1002/aoc.6767>
- Wang, H., Yao, H., Sun, P., Li, D., & Huang, C.-H. (2015). Transformation of tetracycline antibiotics and Fe(II) and Fe(III) species induced by their complexation. *Environmental Science & Technology*, 50(1), 145–153. <https://doi.org/10.1021/acs.est.5b03696>
- Wang, X. Y., Zhu, K. D., Zhu, J., & Ding, S. N. (2021). Photonic crystal of polystyrene nanomembrane: Signal amplification and low triggered potential electrochemiluminescence for tetracycline detection. *Analytical Chemistry*, 93(5), 2959–2967. <https://doi.org/10.1021/acs.analchem.0c04613>
- Wang, Y., Ni, P., Jiang, S., Lu, W., Li, Z., Liu, H., Lin, J., Sun, Y., & Li, Z. (2018). Highly sensitive fluorometric determination of oxytetracycline based on carbon dots and Fe<sub>3</sub>O<sub>4</sub> MNPs. *Sensors and Actuators B: Chemical*, 254, 1118–1124. <https://doi.org/10.1016/j.snb.2017.07.182>
- Wei, F., Cui, X., Wang, Z., Dong, C., Li, J., & Han, X. (2021). Recoverable peroxidase-like Fe<sub>3</sub>O<sub>4</sub>@MoS<sub>2</sub>-ag nanozyme with enhanced antibacterial ability. *Chemical Engineering Journal*, 408, Article 127240. <https://doi.org/10.1016/j.cej.2020.127240>
- Wei, X., Xie, X., Wang, Y., & Yang, S. (2020). Shape-dependent Fenton-like catalytic activity of Fe<sub>3</sub>O<sub>4</sub> nanoparticles. *Journal of Environmental Engineering*, 146(3), Article 04020005. [https://doi.org/10.1061/\(asce\)ee.1943-7870.0001648](https://doi.org/10.1061/(asce)ee.1943-7870.0001648)
- Xiu, F., Lu, Y., Qi, Y., Wang, Y., & He, J. (2021). Ultrasensitive and practical chemiluminescence sensing pesticide residue acetamiprid in agricultural products and environment: Combination of synergistically coupled co-amplifying signal and smart interface engineering. *Talanta*, 235, Article 122811. <https://doi.org/10.1016/j.talanta.2021.122811>
- Yang, W., Weng, C., Li, X., He, H., Fei, J., Xu, W., Yan, X., Zhu, W., Zhang, H., & Zhou, X. (2021). A sensitive colorimetric sensor based on one-pot preparation of h-Fe<sub>3</sub>O<sub>4</sub>@ppy with high peroxidase-like activity for determination of glutathione and H<sub>2</sub>O<sub>2</sub>. *Sensors and Actuators B: Chemical*, 338, Article 129844. <https://doi.org/10.1016/j.snb.2021.129844>
- Zhang, S., Sun, Q., Liu, X., Li, H., Wang, J., & Chen, M. (2022). Ratiometric fluorescence detection of tetracycline for tetracycline adjuvant screening in bacteria. *Sensors and Actuators B: Chemical*, 372, Article 132687. <https://doi.org/10.1016/j.snb.2022.132687>
- Zhang, Y., Mehedi Hassan, M., Rong, Y., Liu, R., Li, H., Ouyang, Q., & Chen, Q. (2022). An upconversion nanosensor for rapid and sensitive detection of tetracycline in food based on magnetic-field-assisted separation. *Food Chemistry*, 373, Article 131497. <https://doi.org/10.1016/j.foodchem.2021.131497>
- Zhang, Y., Zhang, F., Zhou, Y., Zhou, W., Li, S., Zheng, Y., Li, W., Feng, X., & Yuan, M. (2016). Research progress on pretreatment techniques and determination methods of tetracyclines residues in food. *Chinese Journal of Pharmaceutical Analysis*, 36(4), 565–571. <https://doi.org/10.16155/j.0254-1793.2016.04.02>